

Electron microscopy of lead pyroniobate

R. Ubic^{*,†}, I.M. Reaney

Department of Engineering Materials, University of Sheffield, Sheffield, UK

Received in revised form 4 September 2000; accepted 5 October 2000

Abstract

This work investigates the structure and stability of the pyrochlore solid solution $\text{Pb}_n\text{Nb}_2\text{O}_{5+n}$ using a combination of high-resolution electron microscopy and electron diffraction. Single-phase cubic pyrochlore has been obtained for a $\text{Pb}_{1.5}\text{Nb}_2\text{O}_{6.5}$ composition. As expected, compositions containing higher [Pb]/[Nb] ratios showed discreet PbO-rich layers between alternating layers of $\text{Pb}_{1.5}\text{Nb}_2\text{O}_{6.5}$, similar in appearance to Ruddlesden–Popper phases. The occurrence of these layers, which lie along $\langle 111 \rangle_c$ planes, results in a lowering of the overall symmetry to trigonal. These layers and their spacing have a profound effect on the dielectric properties of the ceramics, with a spacing of about 18.3 Å resulting in the most temperature-stable structure. © 2001 Elsevier Science Ltd. All rights reserved.

Keywords: Dielectric properties; Electron microscopy; Niobates; Pyrochlores; X-ray methods

1. Introduction

Microwave resonators are used extensively in telecommunications equipment, including cellular telephones and satellite links and are at the heart of a multi-billion pound market. Auctions in the UK, Germany, and the Netherlands for licenses to run the new generation of mobile phones, the so-called Third Generation or 3G phones, have recently raised a total of \$82.5 billion. Oxide ceramics are critical elements in these microwave devices, and three properties are important in determining their usefulness as dielectric resonators. First, the material must have a high dielectric constant (ϵ_r) to enable size reduction. Second, a high quality factor Q (low $\tan\delta$) means fine frequency tunability and more channels within a given band. Third, these ceramic components play a crucial role in compensating for frequency drift because of their low temperature coefficients of resonant frequency (τ_f). Combining all these properties in a single material is not a trivial problem, and a full understanding of the crystal chemistry of such materials is paramount to future development.

The pyrochlore structure, space group Fd3m (No. 227), is well-understood. Stoichiometrically it is usually written as $\text{A}_2\text{B}_2\text{O}_7$, consisting of large (radius ≈ 1 Å) A-site cation species in 8-fold co-ordination and a network of oxygen octahedra (actually trigonal antiprisms) enclosing smaller (radius ≈ 0.6 Å) B-site cations. The only crystallographic variable is in the 48f oxygen sites, the positions of which have one degree of freedom called x . The cubic form of lead pyroniobate is Pb-deficient, with only 75% of A-sites occupied ($\text{Pb}_{1.5}\text{Nb}_2\text{O}_{6.5}$). Introducing more Pb into this structure causes a rhombohedral distortion of the pyrochlore structure, the nature of which is still not completely understood. For this reason, stoichiometric $\text{Pb}_2\text{Nb}_2\text{O}_7$ does not have the cubic pyrochlore structure.

Cook and Jaffe¹ were the first to report the existence of $\text{Pb}_2\text{Nb}_2\text{O}_7$. Their work showed it to have a distorted fluorite structure of rhombohedral symmetry, $a = 5.285 \pm 0.003$ Å, $\alpha = 89.25^\circ$. In 1972 Brusset et al.² reported observing $\text{Pb}_2\text{Nb}_2\text{O}_7$ as single crystals formed from a melt at 1300°C. The symmetry they reported was monoclinic, with lattice parameters $a = 13.021 \pm 0.012$ Å, $b = 7.483 \pm 0.006$ Å, $c = 34.634 \pm 0.018$ Å, $\beta = 125.18^\circ \pm 0.04$,[‡] and possible space groups C2/m, C2, or Cm.

* Corresponding author. Tel.: +44-20-7882-5160; fax: +44-20-8981 9804.

E-mail address: r.ubic@qmw.ac.uk (R. Ubic).

† Present address: Department of Materials, Queen Mary and Westfield College, London E1 4NS, UK.

‡ JCPDS card No. 30-711 erroneously lists the angle β as 125.3° (mistaking the decimal part of the angle for minutes). This error was not made on the earlier card No. 25-444, which was based on the same work.

Bernotat-Wulf and Hoffmann³ later concluded that $\text{Pb}_2\text{Nb}_2\text{O}_7$ was a trigonal, space group P3m1 (No. 156), with $a=7.472 \text{ \AA}$ and $c=28.351 \text{ \AA}$. Saine et al.⁴ conducted a study of the $\text{PbO-Nb}_2\text{O}_5$ system and found $\text{Pb}_2\text{Nb}_2\text{O}_7$ in both a cubic ($a=10.508 \text{ \AA}$) and rhombohedral ($a=7.464 \text{ \AA}$, $c=18.88 \text{ \AA}$) form, although Wakiya et al.⁵ suggested that full occupancy of the A-site by Pb^{+2} would not be stable in the pyrochlore structure due to its $(6s)^2$ lone pair. Subramanian et al.⁶ calculated that the ratio of cation sizes must fall between 1.4 and 2.2 to form a stable $+2, +5$ pyrochlore. In the case of $\text{Pb}_2\text{Nb}_2\text{O}_7$, this ratio is 2.02, but the effect of the $(6s)^2$ electrons is to cause substantial departure from the centrosymmetric Fd3m space group. Bernotat-Wulf and Hoffmann⁷ published the atomic positions of their $\text{Pb}_2\text{Nb}_2\text{O}_7$ model in 1982. More than a decade later, Leroux et al.⁸ reported a trigonal cell with $a=7.46 \text{ \AA}$, $c=19.2 \text{ \AA}$. Both models are shown in Fig. 1.

2. Procedure

Pellets with compositions in the $\text{Pb}_n\text{Nb}_2\text{O}_{5+n}$ system were prepared by a conventional mixed-oxide route as described elsewhere.⁹ Phase assemblages were checked by scanning electron microscopy (SEM, model JSM 6400, Jeol, Tokyo, Japan) and X-ray diffraction (XRD, model PW1730/10, Philips, Holland) using $\text{CuK}\alpha$ radiation from $10^\circ \leq 2\theta \leq 60^\circ$. Crystallographic para-

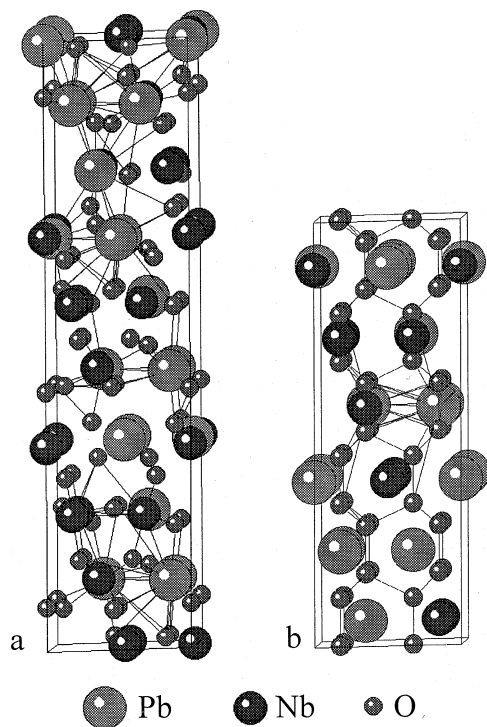


Fig. 1. Crystal models of the $\text{Pb}_2\text{Nb}_2\text{O}_7$ structure as proposed in Refs. 7 (a) and 8 (b), viewed along $\langle 100 \rangle$.

eters of the cubic $\text{Pb}_{1.5}\text{Nb}_2\text{O}_{6.5}$ phase were calculated from high-resolution (0.005°) scans based on the heights and positions of the 111, 311, 222, 400, 440 and 622 peaks obtained from a powder sample carefully back-filled into a holder to minimise texturing. The lattice constant was obtained by a fit to the angular distances between these peaks, correcting for systematic linear error and trigonometric height misalignment, with software developed in-house. The crystallographic x parameter for the 48f oxygen positions was calculated with the same software by measuring the relative intensities of these diagnostic peaks and adjusting the symmetric thermal displacement amplitudes and x parameter until the best fit was found.

Some pellets underwent thinning by conventional ceramographic techniques followed by ion milling (model 600, Gatan, Pleasanton, California, USA) to electron transparency for observation in the transmission electron microscope (TEM, model JEM 3010, Jeol, Japan).

Measurements of τ_f were made at Filtronic Comtek* on a vector network analyser (model 8753E, Hewlett Packard, USA).

3. Results and discussion

3.1. Crystal structure

High-resolution XRD scans of the cubic $\text{Pb}_{1.5}\text{Nb}_2\text{O}_{6.5}$ phase revealed a lattice constant of 10.5604 \AA and a crystallographic x parameter for the 48f oxygen positions

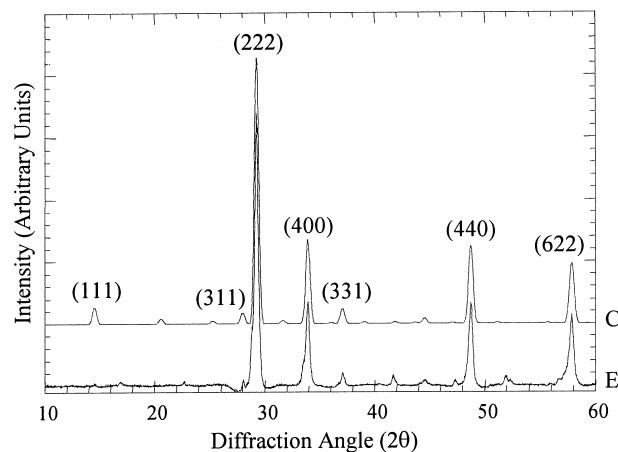


Fig. 2. Calculated (C) and experimental (E) XRD traces for the $\text{Pb}_{1.5}\text{Nb}_2\text{O}_{6.5}$ composition. The conditions for the simulated pattern are $a=10.5604 \text{ \AA}$, $x=0.313$, and the mean square amplitudes of the thermal displacements are $\bar{u}^2(\text{Pb})=0.096 \text{ \AA}^2$, $\bar{u}^2(\text{Nb})=0.008 \text{ \AA}^2$ and $\bar{u}^2(\text{O})=0$.

* Measurements courtesy of Filtronic Comtek, Ceramics Division, Wolverhampton, UK.

of 0.313 (Fig. 2), significantly lower than some authors⁷ have reported but in excellent agreement with later work.^{10,11} For this composition, SADP's can be indexed according to the cubic pyrochlore structure; however, for $n=1.6$, a streaking of intensity is visible along $\langle 111 \rangle$ directions; and for $n > 1.6$, discrete extra reflections appear corresponding to a multiplication of the $\{111\}$ spacing. These defects are visible in the dynamical bright-field images of Fig. 3, which show a $\text{Pb}_{1.6}\text{Nb}_2\text{O}_{6.6}$ grain near a $\langle 111 \rangle$ orientation. Regions of un-defected pyrochlore still remain but are separated by clusters of highly-defective material. Using the invisibility criterion, it can be shown that a different set of defect $\{111\}$ planes is visible in each micrograph. Fig. 4 shows high-resolution images of grains in ceramics with the nominal compositions $\text{Pb}_2\text{Nb}_2\text{O}_7$, $\text{Pb}_{2.2}\text{Nb}_2\text{O}_{7.2}$, and $\text{Pb}_{2.5}\text{Nb}_2\text{O}_{7.5}$. In each case distinct regions, corresponding to a $\langle 110 \rangle$ projection of the pyrochlore structure, are separated and sheared by defect layers. Leroux et al.⁸ suggested that PbO-rich layers may form as planar defects in the lead niobate lattice. The increase in the defect density observed with increasing n (PbO content) points to a similar conclusion.

The images in Fig. 4 show three distinct structures, each one differing by the spacing of the defect layers which seems to decrease with increasing n from infinity for $n=1.5$ (not shown) to 18 \AA for $n=2.0$ to 14 \AA for $n=2.2$ to 9.1 \AA for $n=2.5$.

Simulated XRD patterns corresponding to the crystal models of Refs. 7 and 8 are shown along with an experimental trace for a $\text{Pb}_2\text{Nb}_2\text{O}_7$ pellet in Fig. 5. As is clear, neither model is a very good match. On close inspection and considering the site occupancies reported, Bernotat-Wulf and Hoffmann's "Pb₂Nb₂O₇" model⁷ would actually have the stoichiometry $\text{Pb}_{2.37}\text{Nb}_2\text{O}_{8.82}$, which is not a charge-balanced composition. In addition, the $c=19.2 \text{ \AA}$ axis of Leroux et al.'s⁸ model cannot accommodate the $\approx 27 \text{ \AA}$ spacing clearly observable in the SADP for this composition in Fig. 4a. Finally, high-resolution TEM simulations of these models have so far been unable to reproduce the image in Fig. 4a.

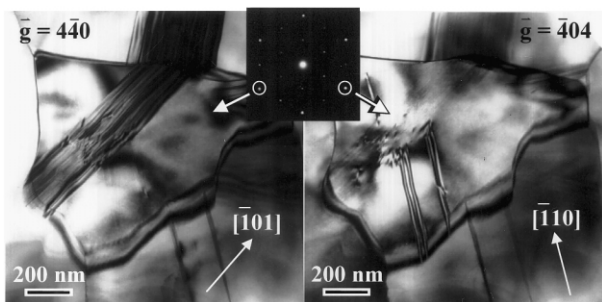
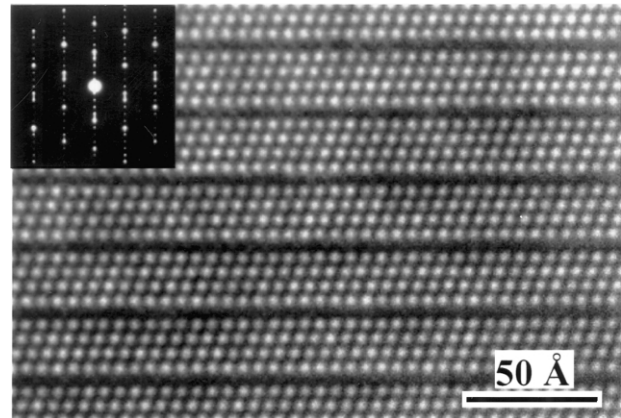


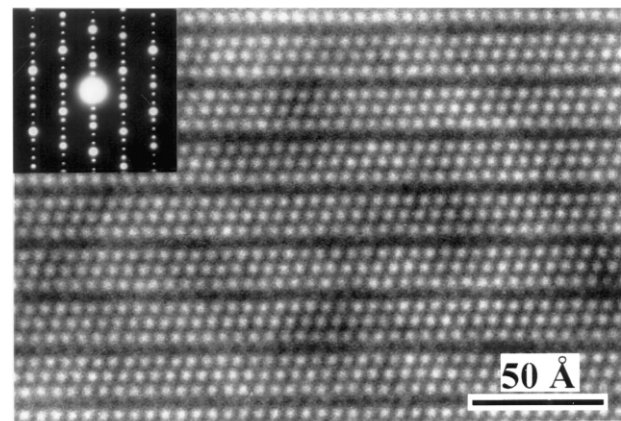
Fig. 3. Dynamical bright-field TEM images of a $\text{Pb}_{1.6}\text{Nb}_2\text{O}_{6.6}$ grain near the $\langle 111 \rangle$ zone.

3.2. Microwave properties

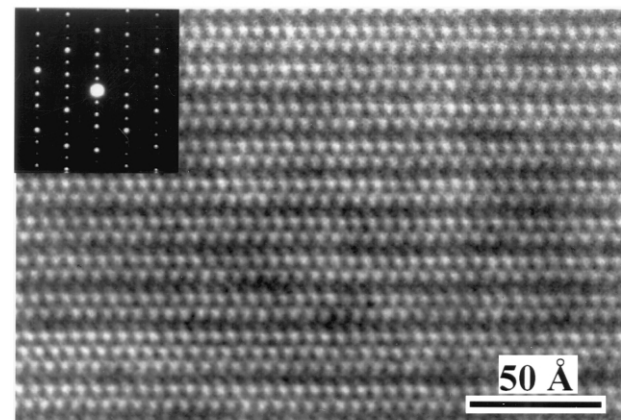
The relationship between τ_f and n is shown in Fig. 6. From $1.5 \leq n \leq 2.0$, τ_f decreased from 1239 to 814 ppm/°C; but increased from $2.0 \leq n \leq 3.0$. The minimum at $n=2.0$ is due either to the effect of the defect layer density or the proximity of the phase transition which occurs at $n=3.0$.



(a)



(b)



(c)

Fig. 4. High-resolution TEM images of grains from ceramics with the nominal compositions (a) $\text{Pb}_2\text{Nb}_2\text{O}_7$, (b) $\text{Pb}_{2.2}\text{Nb}_2\text{O}_{7.2}$, and (c) $\text{Pb}_{2.5}\text{Nb}_2\text{O}_{7.5}$.

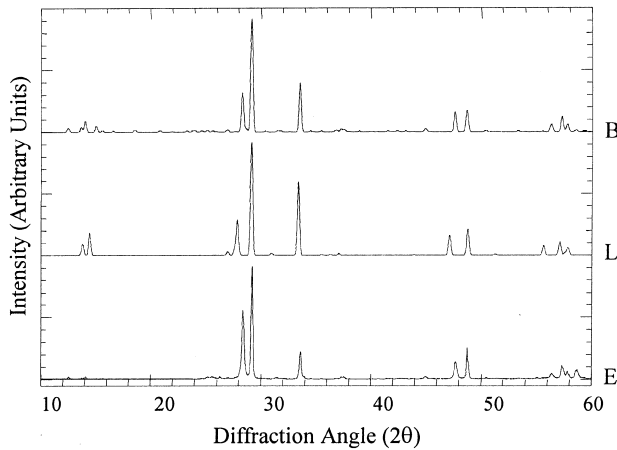


Fig. 5. A comparison of the simulated XRD patterns for the $\text{Pb}_2\text{Nb}_2\text{O}_7$ models proposed by Bernetat-Wulf and Hoffmann⁷ (marked B), Leroux et al.⁸ (marked L), and an experimental trace for a crushed $\text{Pb}_2\text{Nb}_2\text{O}_7$ pellet (marked E).

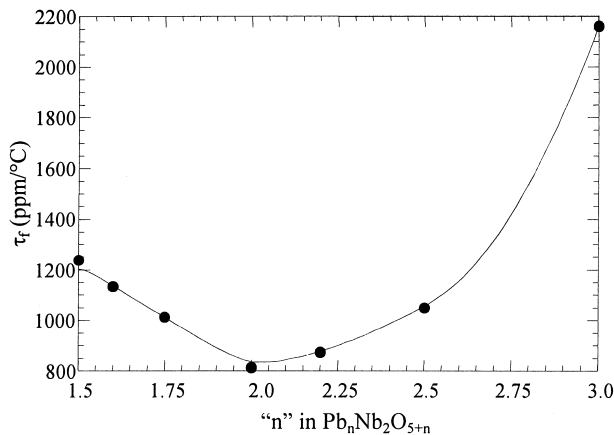


Fig. 6. The variation in τ_r with Pb-content in $\text{Pb}_n\text{Nb}_2\text{O}_{5+n}$.

4. Conclusions

Cubic $\text{Pb}_{1.5}\text{Nb}_2\text{O}_{6.5}$ has the cubic pyrochlore structure, and the x parameter for the 48f oxygen positions is

0.313. For higher concentrations of Pb, there are at least three distinct crystal structures, corresponding to $\text{Pb}_2\text{Nb}_2\text{O}_7$, $\text{Pb}_{2.2}\text{Nb}_2\text{O}_{7.2}$ and $\text{Pb}_{2.5}\text{Nb}_2\text{O}_{7.5}$. Neither of the proposed crystal models of $\text{Pb}_2\text{Nb}_2\text{O}_7$ gives a very good match to experimental data. The $\text{Pb}_2\text{Nb}_2\text{O}_7$ composition yields the most temperature-stable resonators.

References

1. Cook, W. R. Jr. and Jaffe, H., Ferroelectricity in oxides of fluorite structure. *Phys. Rev.*, 1952, **88**(6), 1426.
2. Brusset, H., Mahe, R. and Aung Kyi, U., Caractérisation et comparaison structurales de niobates de type pyrochlore. *C.R. Acad. Sci. C*, 1972, **C275**, 327–330.
3. Bernetat-Wulf, H. and Hoffmann, W., Ein neuartiges Bauprinzip in den Kristallstrukturen der Bleiniobate vom Pyrochlor-Typ. *Naturwissenschaften*, 1980, **67**, 141–142.
4. Saine, M. C., Gasperin, M. and Brusset, H., Étude Cristallographique de Cinq Phases de Niobates de Plomb Dérivant de la Structure Pyrochlore. *Rev. Chim. Min.*, 1981, **18**, 587–592.
5. Wakiya, N., Kim, B.-H., Shinozaki, K. and Mizutani, N., Composition range of cubic pyrochlore type compound in lead-magnesium-niobium-oxygen system. *J. Ceram. Soc. Jpn.*, 1994, **102**(6), 612–615.
6. Subramanian, M. A., Aravamudan, G. and Subba Rao, G. V., Oxide pyrochlores — a review. *Prog. Solid State Chem.*, 1983, **15**(2), 55–144.
7. Bernetat-Wulf, H. and Hoffmann, W., Die Kristallstrukturen der Bleiniobate vom Pyrochlor-Typ. *Z. Kristallogr.*, 1982, **158**, 101–117.
8. Leroux, Ch., Tatarenko, H. and Nihoul, G., High-resolution electron microscopy modelling of homologous series in non-stoichiometric lead-niobium oxides. *Phys. Rev. B: Condens. Matter*, 1996, **53**(18), 11993–12005.
9. Ubic, R. and Reaney, I. M., Lead niobate ceramics for microwave dielectric resonators. In *Electronic Ceramic Materials and Devices*, Vol. 106, ed. K. M. Nair and A. S. Bhalla. American Ceramic Society, Westerville, OH, 2000, pp. 263–275.
10. Beech, F., Jordan, W. M., Catlow, C. R., Santoro, A. and Steele, B. C. H., Neutron powder diffraction structure and electrical properties of the defect pyrochlores $\text{Pb}_{1.5}\text{M}_2\text{O}_{6.5}$ ($\text{M} = \text{Nb}, \text{Ta}$). *J. Solid State Chem.*, 1988, **77**, 322–335.
11. Wakiya, N., Saiki, A., Ishizawa, N., Shinozaki, K. and Mizutani, N., Crystal growth, crystal structure and chemical composition of a pyrochlore type compound in lead-magnesium-niobium-oxygen system. *Mater. Res. Bull.*, 1992, **28**, 137–143.